Inorg. Chem. **2002**, *41*, 5052–5058

Synthesis and Characterization of Novel Homoleptic *N,N*-Dialkylcarbamato Complexes of Antimony: Precursors for the Deposition of Antimony Oxides

Graeme A. Horley, Mary F. Mahon, and Kieran C. Molloy*

Department of Chemistry, University of Bath, Claverton Down, Bath BA2 7AY, United Kingdom

Peter W. Haycock and Christopher P. Myers

Birchall Centre for Inorganic Chemistry and Materials Science, School of Chemistry and Physics, Lennard-Jones Laboratories, Keele University, Staffordshire ST5 5BG, United Kingdom

Received April 15, 2002

A series of tris(*N*,*N*-dialkylcarbamato)antimony(III) complexes, $Sb(O_2CNR_2)_3$ (R = Me, Et, Pr^i), have been synthesized and are the first members of this class of compound to have been crystallographically characterized. $Sb(O_2CNMe_2)_3$ (**1**) exists as a weakly bound dimer, whereas its diethyl and diisopropyl analogues (**2**, **3**) are monomeric. In addition, tetrakis(*N*,*N*-diethylcarbamato)tin(IV) (**4**) has been prepared for comparison and shown by single-crystal X-ray analysis to exhibit the relatively rare SnO_8 coordination. Crystallographic data: for **1**, $a = 8.7520(5)$ Å, $b = 14.2970(8)$ Å, $c = 11.8150(7)$ Å, $\beta = 108.029(2)°$, monoclinic, $P2_1/c$, $Z = 4$; for **2**, $a = b = 14.4690(2)$ Å, $c = 16.6740(2)$ Å, trigonal, $R\bar{3}$, $Z = 6$; for **3**, $a = 11.9881(2)$ Å, $b = 11.6521(3)$ Å, $c = 19.8780(6)$ Å, $\beta = 90.401(1)°$, monoclinic, $P2_1/n$, $Z = 4$; for **4**, $a = 13.9654(2)$ Å, $b = 12.0817(2)$ Å, $c = 16.6752(2)$ Å, $\beta = 108.1960(7)°$, monoclinic, $C2/c$, $Z = 4$. $Sb(O_2CNMe_2)_3$ has been used as a single-source precursor in the low-pressure chemical vapor deposition of the senarmonite form of Sb_2O_3.

Introduction

There is currently much interest in the preparation of metal oxide materials, which are utilized in a variety of technological applications including microelectronics,[1,2] ceramics,[3] coatings,[4,5] catalysis,[6,7] and gas sensors.[8,9] The desire to prepare such materials has led to the accelerated development of precursor chemistry and the utilization of a number of deposition techniques to prepare oxides as films (generally by variations on chemical vapor deposition technologies),[10] or in nanoparticulate form by sol−gel routes.[11,12]

Our own interest centers on the deposition of antimony oxide thin films,[13] which have been shown to have potential applications in many areas including their components of electronic ceramics, heterogeneous catalysis,[14,15] and sensors.[16] Our aim is to prepare novel single-source precursors for the deposition of antimony oxide by metal−organic chemical vapor deposition (MOCVD), where an attractive precursor possesses the attributes of being reasonably volatile, having a clean decomposition pathway, and by utilizing the single-source technique, having a low tendency to prereaction. We have already reported that homoleptic antimony(III) alkoxides can be used to deposit thin films of

* Author to whom correspondence should be addressed. E-mail: chskcm@bath.ac.uk.

(1) Gordon, R. G.; Becker, J.; Hausmann, D.; Suh, S. *Chem. Mater.* **2001**, *13*, 2463.
(2) Senzaki, Y.; Hochberg, A. K.; Norman, J. A. T. *Adv. Mater. Opt. Electron.* **2000**, *10*, 93.
(3) Kleveland, K.; Einarsrud, M. A.; Grande, T. *J. Am. Ceram. Soc.* **2000**, *83*, 3158.
(4) Ballard, R. L.; Williams, J. P.; Njus, J. M.; Kiland, B. R.; Soucek, M. D. *Eur. Polym. J.* **2001**, *37*, 381.
(5) Taylor, D. J.; Fleig, P. F.; Schwab, S. T.; Page, R. A. *Surf. Coat. Technol.* **1999**, *120*−*121*, 465.
(6) Burcham, L. J.; Briand, L. E.; Wachs, I. E. *Langmuir* **2001**, *17*, 6164.
(7) Park, J. S.; Doh, D. S.; Lee, K. Y. *Top. Catal.* **2000**, *10*, 127.
(8) Kiss, G.; Pintér, Z.; Preczel, I. V.; Sassi, Z.; Réti, F. *Thin Solid Films* **2001**, *391*, 216.
(9) Dusastre, V.; Williams, D. E. *J. Mater. Chem.* **1999**, *9*, 445.
(10) Jones, A. C. *Chem. Soc. Rev.* **1997**, *26*, 101.
(11) Livage, J.; Ganguli, D. *Sol. Energy Mater.* **2001**, *68*, 365.
(12) Vioux, A. *Chem. Mater.* **1997**, *9*, 2292.
(13) Haycock, P. W.; Horley, G. A.; Molloy, K. C.; Myers, C. P.; Rushworth, S. A.; Smith, L. M. *Chem. Vap. Deposition* **2001**, *7*, 191.
(14) Centi, G.; Perathoner, S. *Appl. Catal.* **1995**, *124A*, 317.
(15) Grasselli, R. K.; Burrington, J. D. *Adv. Catal.* **1981**, *30*, 133.
(16) Haycock, P. W.; Horley, G. A.; Molloy, K. C.; Myers, C. P.; Rushworth, S. A.; Smith, L. M. *J. Phys. IV* **2001**, *11*, Pr3.

10.1021/ic0202716 CCC: $22.00
Published on Web 08/30/2002

Sb_2O_3 (senarmonite) and Sb_6O_{13} depending on growth conditions,[13] and we have prepared novel complexes of the form $Sb(OR)_n$ ($n = 3, 5$) which are the first crystallographically authenticated examples of monomeric Sb(III) and Sb(V) alkoxide structures.[17] We now look to utilize alternative ligand systems to prepare novel precursors.

Single-source metal oxide precursor chemistry has been dominated by the use of alkoxides, β-diketonates, carboxylates, and heteroleptic compounds involving mixtures of these ligands.[10,18] *N*,*N*-Dialkylcarbamato-metal complexes, $[M(O_2CNR_2)_n]_m$, have, however, received little attention as MOCVD precursors, in contrast to the related *N*,*N*-dialkyldithiocarbamato-($[M(S_2CNR_2)_n]_m$), *N*,*N*′-dialkylmonothiocarbamato-($[M(OSCNR_2)_n]_m$), and *N*,*N*′-dialkyldiselenocarbamato-metal complexes ($[M(Se_2CNR_2)_n]_m$)[18,19] which have been shown to be excellent precursors for the deposition of semiconducting chalcogenide materials. The structural chemistry of metal carbamates is somewhat better developed, led by the work of Calderazzo and co-workers,[20−22] and derivates of a wide range of metals have been reported. There are, however, no reports of homoleptic tris(*N*,*N*-dialkylcarbamato)antimony(III) complexes in the literature, although Meinema and Noltes reported the preparation of $RSb(O_2CNEt_2)_2$ (R = Et, Bu^n, Ph) over thirty years ago.[23]

In this paper we report the synthesis and characterization of $Sb(O_2CNR_2)_3$ [R = Me (**1**), Et (**2**), Pr^i (**3**)], each of which has been analyzed by single-crystal X-ray diffraction. In addition, we have prepared tetrakis(*N*,*N*-diethylcarbamato)-tin(IV), $Sn(O_2CNEt_2)_4$ (**4**), as a potentially novel single-source precursor for the deposition of tin oxide thin films, which have many of the same applications as the analogous antimony oxide materials. Experiments which test the potential of **1** as a representative compound for use in CVD experiments are also included.

Experimental Section

General Procedures. Elemental analyses were performed with an Exeter Analytical CE 440 analyzer, though it only proved possible to obtain accurate data for compound **1** due to the air-sensitivity of the remaining species. ^{1}H, ^{13}C, and ^{119}Sn NMR spectra were recorded on a Bruker Avance 300 MHz FT-NMR spectrometer, using saturated C_6D_6 solutions at room temperature. SEM was carried out on a JEOL JSM-6310 microscope while quantitative EDAX measurements were made on a JEOL JXA-8600 electron probe microanalyzer. XRD was performed with either a Bruker D8 or a Phillips 1310 diffractometer on which coupled $\theta-2\theta$ scans were carried out. Thermogravimetric studies were performed on a Perkin-Elmer TGA7 analyzer; samples were loaded as quickly as possible in air then the temperature was increased under a flow of dry N_2 gas.

$Sb(NMe_2)_3$ (Strem), $SbCl_3$, $Sn(NEt_2)_4$, anhydrous Et_2NH, and anhydrous Pr^i_2NH (all Aldrich) were purchased and used as supplied. Dry CO_2 was supplied by BOC. Hexane and toluene were distilled over CaH_2 prior to use. All reactions were carried out in an inert atmosphere (N_2 and Ar) using a drybox and Schlenk-line techniques. Melting points were recorded in sealed glass capillary tubes with a Gallenkamp melting point apparatus.

Synthesis of Tris(*N*,*N*-dimethylcarbamato)antimony(III), $Sb(O_2CNMe_2)_3$ (1): Tris(*N*,*N*-dimethylamino)antimony(III) (1.00 g, 3.94 mmol) was transferred to a Schlenk tube and diluted with dry hexane (30 mL). Into a single-necked round-bottomed flask was placed dry ice (CO_2) pellets, and a cannula was passed between the two vessels. CO_2 vapor was then passed into the solution, causing an immediate exothermic response and the appearance of a white solid material. The CO_2 was allowed to bubble through the solution for 30 min, until the flask had returned to room temperature. The solvent was then removed in vacuo and the resulting fine white powder was recrystallized from toluene at −20 °C to yield colorless crystals (1.38 g, 91%). Mp: 108 °C. Anal. Found (calcd for $C_9H_{18}O_6N_3Sb$): C 25.5 (28.0); H 4.52 (4.70); N 10.14 (10.89). ^{1}H NMR δ 2.57 (s, 18H, CH_3); ^{13}C NMR δ 34.5 (CH_3), 161.8 (C−N). IR (Nujol): 1377, 1258, 1026, 846, 783, 713, 640 cm^{-1}.

Synthesis of Tris(*N*,*N*-diethylcarbamato)antimony(III), $Sb(O_2CNEt_2)_3$ (2): Antimony(III) chloride (2.70 g, 11.84 mmol) was dissolved in dry toluene (30 mL) in a round-bottomed flask under argon. In another vessel, distilled diethylamine (7.34 mL, 5.19 g, 70.95 mmol) was diluted in dry toluene (20 mL) and the solution added dropwise to the $SbCl_3$ solution; a slight warming and a white coloration were observed. The mixture was stirred for 20 min and then CO_2 vapor was bubbled through the mixture for *ca*. 45 min until the reaction flask had returned to room temperature. After being allowed to settle, the solution was separated by filtration and the solvent removed in vacuo to give a waxy off-white material which, when stirred in dry hexane (20 mL) for 10 min and dried again in vacuo, became a white powder. The powder was redissolved in the minimum quantity of toluene and placed in a freezer, yielding colorless crystals (yield 3.83 g, 69%). Mp: 131−2 °C. ^{1}H NMR δ 0.95 (t, 18H, CH_3, J = 7.2 Hz), 3.09 (q, 12H, CH_2, J = 7.2 Hz); ^{13}C NMR δ 14.1 (CH_3), 41.8 (CH_2), 163.2 (C−N). IR (Nujol): 1605, 1374, 1288, 1195, 1075, 970, 936, 830, 779, 727, 694, 660, 593 cm^{-1}.

Synthesis of Tris(*N*,*N*-diisopropylcarbamato)antimony(III), $Sb(O_2CNPr^i_2)_3$ (3): The same synthetic procedure as described for **2** was followed, using antimony(III) chloride (1.80 g, 7.89 mmol) dissolved in dry toluene (30 mL) and anhydrous diisopropylamine (6.65 mL, 4.80 g, 47.45 mmol). Recrystallization from toluene yielded colorless crystals of the title compound (yield 2.95 g, 70%). Mp: 139 °C. ^{1}H NMR δ 1.16 (s, 9H, CH_3), 1.18 (s, 9H, CH_3), 3.81 (s, 3H, C−H); ^{13}C NMR δ 19.4 (CH_3), 45.2 (C−H); 161.2 (C−N).

Synthesis of Tetrakis(*N*,*N*-diethylcarbamato)tin(IV), $Sn(O_2CNEt_2)_4$ (4): Tetrakis(*N*,*N*-diethylamino)tin(IV) (1.52 g, 3.73 mmol) was placed in a Schlenk tube and diluted in dry hexane (30 mL). CO_2 vapor was then bubbled through the solution for 1 h, by which time a white solid product had been formed, which was isolated by removing the hexane under reduced pressure. The powder was very soluble in toluene and the minimum amount (less than 10 mL) was used to redissolve the product. The solution was placed cooled at −20 °C for 48 h, affording colorless platelike crystals (yield 1.61 g, 74%). Mp: 120−121 °C. ^{1}H NMR δ 0.94

(17) Haycock, P. W.; Horley, G. A.; Molloy, K. C.; Myers, C. P. *Inorg. Chem.* **2002**, *41*, 1652.
(18) Gleizes, A. N.; *Chem. Vap. Deposition* **2000**, *6*, 155.
(19) Horley, G. A.; Lazell, M. R.; O'Brien, P. *Chem. Vap. Deposition* **1999**, *5*, 203.
(20) Abram, U.; Belli Dell'Amico, D.; Calderazzo, F.; Marchetti, L.; Strähle, J. *J. Chem. Soc., Dalton Trans.* **1999**, 4093.
(21) Belli Dell'Amico, D.; Boschi, D.; Calderazzo, F.; Ianelli, S.; Labella, L.; Marchetti, F.; Pelizzi, G.; Quadrelli, E. G. F. *Inorg. Chim. Acta* **2000**, *300−302*, 882.
(22) Belli Dell'Amico, D.; Calderazzo, F.; Ianelli, S.; Labella, L.; Marchetti, F.; Pelizzi, G. *J. Chem. Soc., Dalton Trans.* **2000**, 4339.
(23) Meinema, H. A.; Noltes, J. G. *J. Organomet. Chem.* **1970**, *25*, 139.

Table 1. Crystallographic Data for **1**−**4**

	1	**2**	**3**	**4**
empirical formula	$C_9H_{18}N_3O_6Sb$	$C_{15}H_{30}N_3O_6Sb$	$C_{21}H_{42}N_3O_6Sb$	$C_{20}H_{40}N_4O_8Sn$
fw	386.01	470.17	554.33	583.25
cryst syst	monoclinic	trigonal	monoclinic	monoclinic
space group	$P2_1/c$	$R\bar{3}$	$P2_1/n$	$C2/c$
a, Å	8.7520(5)	14.4690(2)	11.9881(2)	13.9654(2)
b, Å	14.2970(8)	14.4690(2)	11.6521(3)	12.0817(2)
c, Å	11.8150(7)	16.6740(2)	19.8780(6)	16.6752(2)
β, deg	108.029(2)		90.401(1)	108.1960(7)
vol, Å^3	1405.8(1)	3023.06(7)	2776.6(1)	2672.84(7)
Z	4	6	4	4
radiation used, λ (Å)	Mo Kα 0.71070	Mo Kα 0.71070	Mo Kα 0.71070	Mo Kα 0.71070
μ(Mo Kα), mm^{-1}	1.988	1.402	1.029	1.003
density, ρ(calcd) (mg/m^3)	1.298	1.550	1.326	1.449
independent reflns	3855 [R(int) = 0.0352]	1955 [R(int) = 0.0494]	5662 [R(int) = 0.0665]	3885 [R(int) = 0.0512]
final R indices	$R_1 = 0.0276$	$R_1 = 0.0196$	$R_1 = 0.0618$	$R_1 = 0.0257$
[$I > 2\sigma(I)$]	$wR_2 = 0.0651$	$wR_2 = 0.0460$	$wR_2 = 0.1302$	$wR_2 = 0.0613$
R indices (all data)	$R_1 = 0.0395$	$R_1 = 0.0211$	$R_1 = 0.0787$	$R_1 = 0.0317$
	$wR_2 = 0.0732$	$wR_2 = 0.0467$	$wR_2 = 0.1366$	$wR_2 = 0.0639$

Table 2. Selected Metrical Data for **4**

Bond Lengths, Å			
Sn(1)−O(1)	2.156(1)	Sn(1)−O(3)	2.163(1)
Sn(1)−O(2)	2.209(1)	Sn(1)−O(4)	2.196(1)
Bond Angles (deg)			
O(1)−Sn(1)−O(2)	60.23(4)	O(2)−Sn(1)−O(4)	133.27(4)
O(1)−Sn(1)−O(3)	86.71(4)	O(2)−Sn(1)−O(2')	75.17(4)
O(1)−Sn(1)−O(4)	84.41(4)	O(2)−Sn(1)−O(3')	81.24(4)
O(1)−Sn(1)−O(1')	165.27(4)	O(2)−Sn(1)−O(4')	124.70(4)
O(1)−Sn(1)−O(2')	134.40(4)	O(3)−Sn(1)−O(4)	60.30(4)
O(1)−Sn(1)−O(3')	95.30(4)	O(3)−Sn(1)−O(3')	164.35(4)
O(1)−Sn(1)−O(4')	83.95(4)	O(3)−Sn(1)−O(4')	135.32(4)
O(2)−Sn(1)−O(3)	86.36(4)	O(4)−Sn(1)−O(4')	75.32(4)

Table 3. Selected Metrical Data for **1**−**3**

	1	**2**[a]	**3**
bond lengths, Å			
Sb(1)−O(1)	2.045(2)	2.0421(9)	2.016(4)
Sb(1)−O(2)	2.541(2)	2.5966(9)	2.586(4)
Sb(1)−O(3)	2.051(2)		2.092(4)
Sb(1)−O(4)	2.630(2)		2.493(4)
Sb(1)−O(5)	2.035(2)		2.076(4)
Sb(1)−O(6)	2.898(2)		2.495(4)
Sb(1)−O(6')	2.769(2)		
bond angles (deg)			
O(1)−Sb(1)−O(2)	56.70(7)	55.86(3)	55.9(1)
O(1)−Sb(1)−O(3)	83.69(7)	86.13(4)[a]	87.7(2)
O(1)−Sb(1)−O(4)	137.03(6)	140.81(3)	79.3(1)
O(1)−Sb(1)−O(5)	80.83(7)		87.9(2)
O(1)−Sb(1)−O(6)	119.54(6)	86.45(3)	79.6(1)
O(2)−Sb(1)−O(3)	81.96(7)		128.7(1)
O(2)−Sb(1)−O(4)	120.16(5)	119.81(3)	80.0(1)
O(2)−Sb(1)−O(5)	137.15(7)		128.8(1)
O(2)−Sb(1)−O(6)	155.93(5)		79.7(1)
O(3)−Sb(1)−O(4)	55.12(6)		56.7(1)
O(3)−Sb(1)−O(5)	86.01(6)		76.9(2)
O(3)−Sb(1)−O(6)	79.65(5)		132.4(1)
O(4)−Sb(1)−O(5)	122.06(6)		132.0(1)
O(4)−Sb(1)−O(6)	88.61(8)		156.5(1)
O(5)−Sb(1)−O(6)	50.61(6)		57.0(1)

[a] O(3) ≡ O(1′), O(4) ≡ O(2′), O(5) ≡ O(1″), O(6) ≡ O(2″).

(t, 12H, CH_3, $J = 7.0$ Hz), 3.09 (q, 8H, $-CH_2$, $J = 7.0$ Hz); ^{13}C NMR δ 13.9 (CH_3), 42.9 (CH_2), 166.2 (C−O); ^{119}Sn NMR δ −930.0. IR (Nujol): 1612, 1205, 1073, 976, 853, 793, 722, 640 cm^{-1}.

Crystal Structures. Experimental details relating to the single-crystal X-ray crystallographic study of complexes **1**−**4** are given in Table 1. Data were collected on a Nonius Kappa CCD diffractometer at 150 K. The refinement method was full-matrix least-squares on F^2. In all cases a semiempirical absorption correction from equivalents was made. Hydrogen atoms were included at calculated positions.

In the case of **3**, isopropyl groups containing C(2), C(3), and C(4) were disordered in 65:35 ratio with C(2A), C(3A), and C(4A). Two large residual peaks remained at the conclusion of refinement, with the largest proximate to Sb(1). The crystal was of mediocre quality.

The asymmetric units of **1**−**4** are shown in Figures 1−4, respectively. For **3**, only the major component of the disorder described above is shown for clarity.

CVD Studies. The hot-wall LP-CVD apparatus used in the deposition experiments (see Chart 1) comprises a horizontally mounted silica glass reactor tube (30 cm long, 3 cm internal diameter) with one end placed inside a cylindrical tube furnace (Elite Thermal Systems Ltd.) that is used to volatilize the precursor material (ca. 100−250 mg per run). The substrate (borosilicate glass slide) is placed on a sloping graphite susceptor block (10 cm long, max height 2.5 cm; Morgan Speciality Graphite) that is pushed into position by connection to a thermocouple housed within the glass tube stopper, which seals tight with an O-ring connection. A second, smaller O-ring connects a glass tap (J. Young) to the reactor tube, allowing a vacuum line (Leybold Trivac D5-E pump system, 10^{-2} Torr) to be attached. The substrate is then heated by raising a bevelled ceramic heater (Infrared Salamander) to the underside of the reactor tube. The precursor was heated to 130 °C and deposition allowed to proceed over a 15-min period, at 10^{-2} Torr with the glass substrate heated to 380 °C (the ceramic heater set to 500 °C).

Results and Discussion

$Sb(O_2CNMe_2)_3$ (**1**) was prepared by the insertion of CO_2 into the Sb−N bonds of commercially available $Sb(NMe_2)_3$, a process that is highly exothermic.

$$Sb(NMe_2)_3 + 3CO_2 \rightarrow Sb(O_2CNMe_2)_3 \qquad (1)$$

A single resonance in the ^{1}H NMR spectrum of **1** suggests that all the methyl protons are equivalent and that **1** is monomeric in solution. The complex is soluble in most organic solvents and was easily dissolved in dry toluene, from which clear, air-sensitive crystals were obtained on cooling.

Chart 1

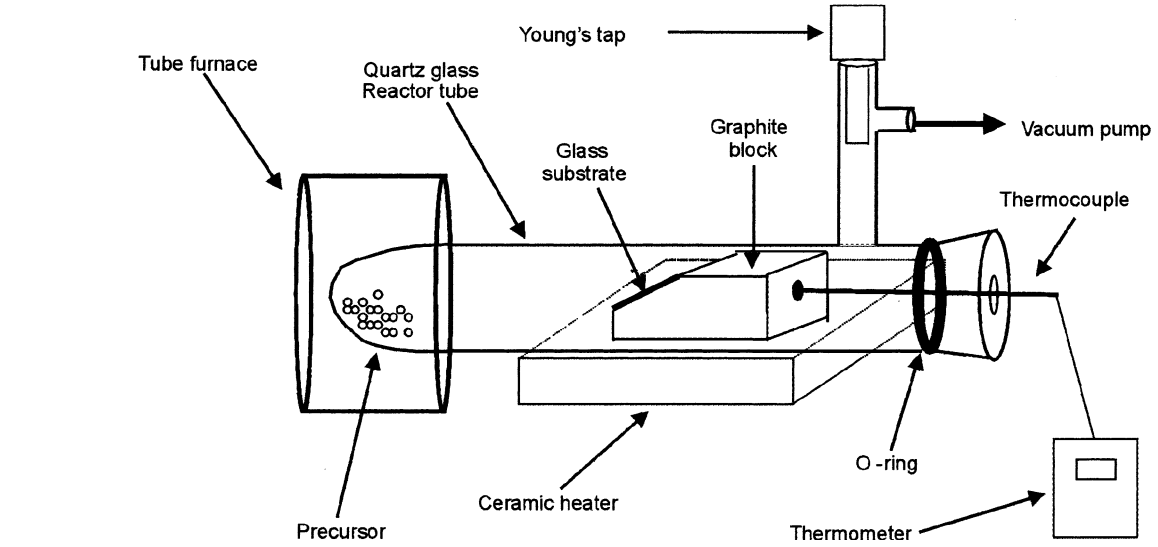

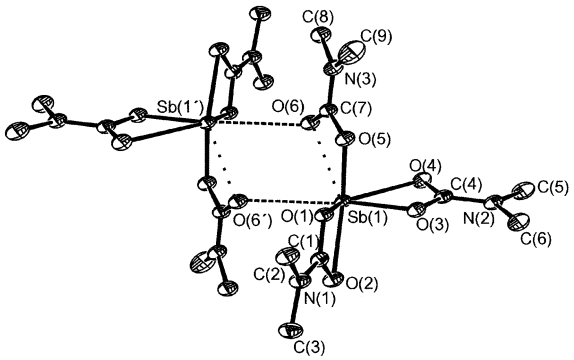

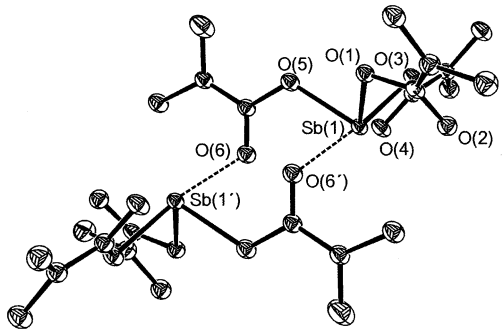

Figure 1. (a) The dimeric structure of **1** showing the asymmetric unit and the labeling scheme. Ellipsoids are at the 30% probability level. The lower orientation (b) shows the non-planar nature of the dimer.

$Sb(O_2CNEt_2)_3$ (**2**) and $Sb(O_2CNPr^i_2)_3$ (**3**) were synthesized by the following route:

$$SbCl_3 + 6R_2NH \rightarrow Sb(NR_2)_3 + 3R_2NH_2Cl$$

$$Sb(NR_2)_3 + 3CO_2 \rightarrow Sb(O_2CNR_2)_3$$

$$R = Et\ (\mathbf{2}),\ Pr^i\ (\mathbf{3})$$

In this procedure, the tris(amido)antimony(III) is generated in situ; the dialkylammonium salt produced when the secondary amine is added to the $SbCl_3$ solution is insoluble

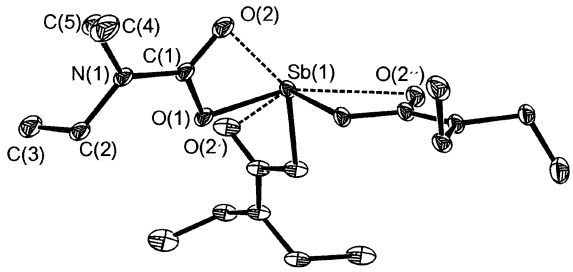

Figure 2. The structure of **2** showing the asymmetric unit and the labeling scheme. Ellipsoids are at the 30% probability level.

in toluene and does not interfere with the subsequent reaction with CO_2. Compounds **2** and **3** were isolated as white, air-sensitive powders, which could be re-crystallized from toluene. As for **1**, the NMR spectra for **2** and **3** suggest that all of the ligands are equivalent and, by implication, that complexes are monomeric in solution.

For comparison, the homoleptic tin species, $Sn(O_2CNEt_2)_4$ (**4**) was prepared similarly to **1**:

$$Sn(NEt_2)_4 + 4\ CO_2 \rightarrow Sn(O_2CNEt_2)_4\ (\mathbf{4})$$

Compound **4** has been prepared previously, but no spectral data have been quoted.[24] The ^{119}Sn NMR chemical shift (−930.0 ppm) is similar to that reported for $Sn(O_2CNPr^i_2)_4$ (−920.8 ppm).[24] It appears more stable than the antimony analogues, but still requires storage under anaerobic conditions, and is soluble in common organic solvents.

The facile nature of the weight loss inherent in all four compounds (see thermal decomposition studies, below) has made accurate microanalysis of the samples difficult. However, the ^1H and ^{13}C NMR spectra of all four compounds show no additional peaks other than those expected, save in the case of **2** where traces of hexane and toluene are visible.

The single-crystal X-ray structure of **1** (Figure 1) indicates that in the solid state the complex is dimeric in nature, with

(24) Abis, L.; Belli Dell'Amico, D.; Calderazzo, F.; Caminiti, R.; Garbassi, F.; Pelizzi, G.; Robino, P.; Tomei, A. *J. Mol. Catal. A* **1966**, *108*, L113.

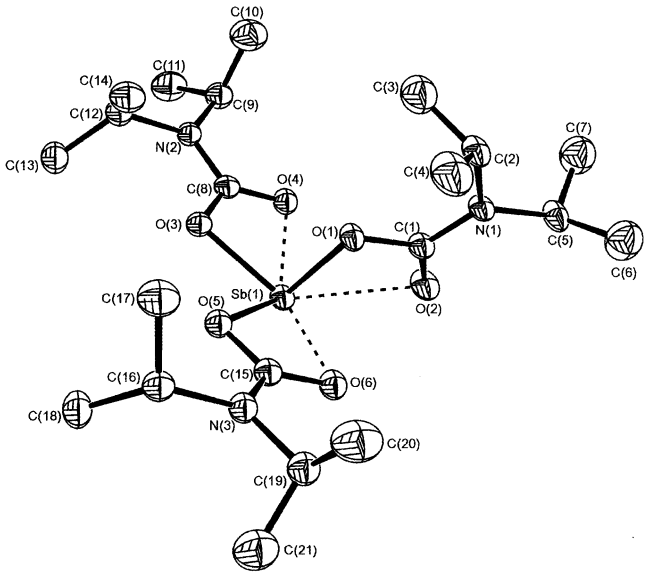

Figure 3. The structure of **3** showing the asymmetric unit and the labeling scheme. Ellipsoids are at the 30% probability level.

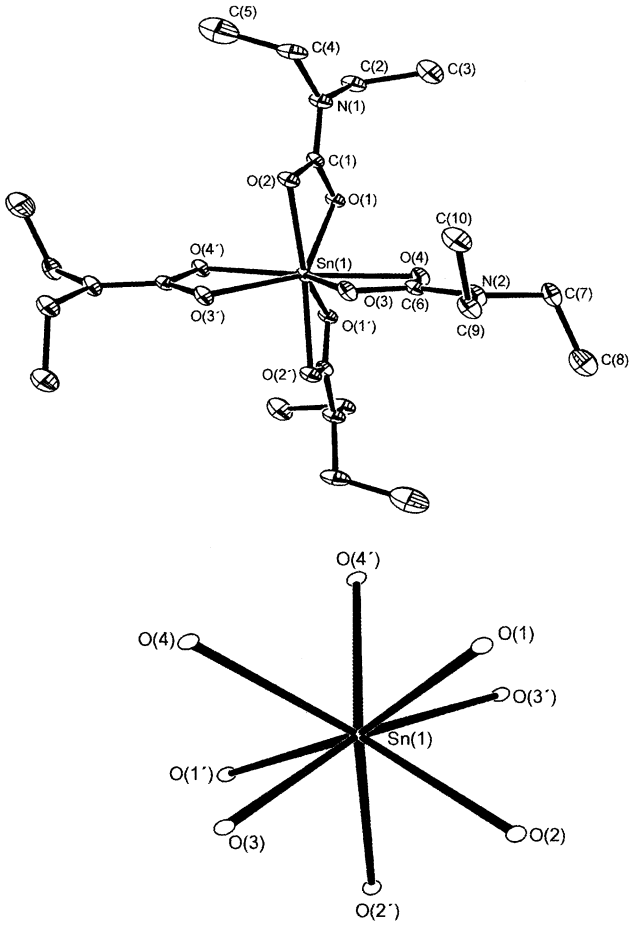

Figure 4. The structure of **4** showing (top) the asymmetric unit and the labeling scheme (ellipsoids are at the 30% probability level) and (bottom) highlighting the square antiprism coordination about tin.

short intermolecular contacts between the Sb of one unit and an oxygen atom of one of the *N*,*N*-dimethylcarbamato ligands of its neighbor. This intermolecular interaction [Sb(1)−O(6′) = 2.769(2) Å] is significantly shorter than the corresponding intramolecular contact [Sb(1)−O(6) = 2.898(2) Å]. Taken

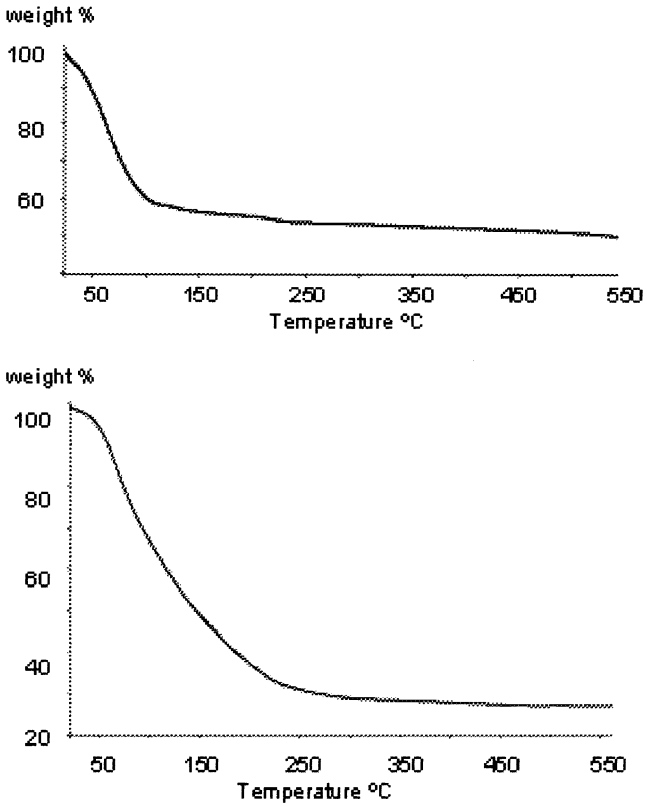

Figure 5. TGA traces for **1** (top) and **4** (bottom).

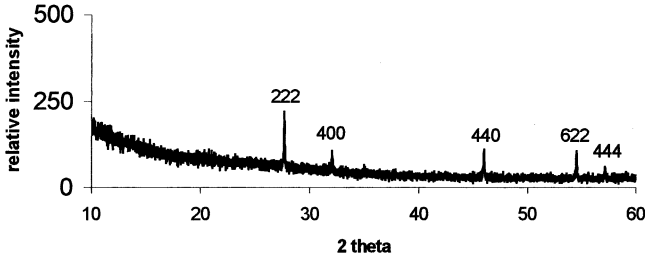

Figure 6. XRD pattern of the residue obtained from TGA of **1**, identified as Sb_2O_3 (senarmonite) (JCPDS 05-0534)

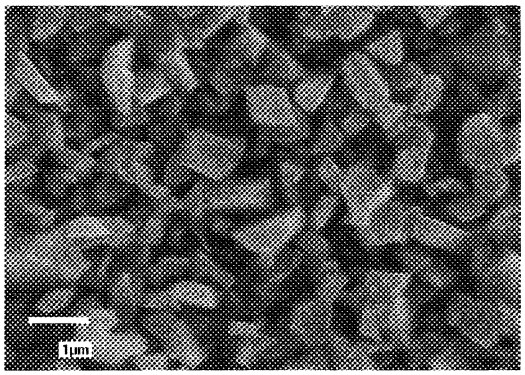

Figure 7. SEM of the Sb_2O_3 (senarmonite) film obtained from LPCVD with use of **1** as precursor.

as a whole, there are three short and three long Sb−O interactions at each Sb center, a motif often seen with complexes of this type. The local geometry about each antimony is similar to those found in **2** and **3**, while the lone pairs on each antimony are parallel to each other (Figure 1b). The magnitude of these interactions [2.04−2.05 Å (short); 2.54−2.90

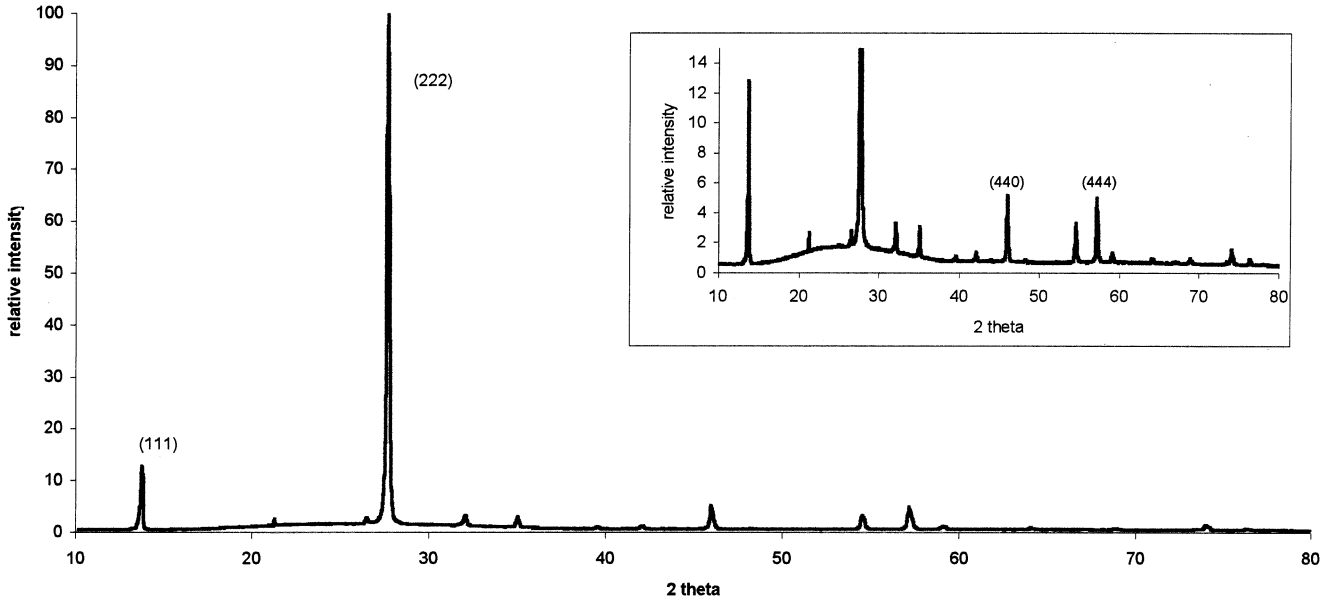

Figure 8. XRD pattern of the film obtained from LPCVD with use of **1** as precursor, identified as Sb_2O_3 (senarmonite) (JCPDS 05-0534).

Å (long)] is comparable to those found in the tris(acetato)-antimony(III) complex [2.02−2.09 Å (short) and 2.60−2.77 Å (long)].[25] However, this latter complex only exhibits one close intermolecular contact per pair of molecules, giving rise to a polymeric chain. In **1** there are two such interactions per pair, thus affording the dimeric structure.

However, in contrast to **1**, the structures of **2** and **3** (Figures 2 and 3) show that both complexes are monomeric in the solid state, presumably due to the steric effect of the larger alkyl moieties. In neither case are there any intermolecular contacts involving antimony and either oxygen or nitrogen which are <4 Å. Complex **2** crystallizes in the trigonal $R\bar{3}$ space group, hence there is 3-fold symmetry at the Sb center. There are three short [Sb(1)−O(1) = 2.042(1) Å] and three long [Sb(1)−O(2) = 2.597(1) Å] Sb−O bonds such that chelation by the carbamate is highly asymmetric. Figure 2 shows that the geometry about antimony is pyramidal with a clearly visible vacant site occupied by a stereochemically active lone electron pair, if only the short Sb−O bonds are considered. The Sb(1)−O(2) interaction is, however, short enough to be considered real, and as such the coordination sphere about the metal is best described as octahedral, distorted by the presence of the lone pair into a *pseudo*-seven-coordinated arrangement. The grouping of the short Sb−O bonds below the lone pair site with the longer chelating Sb−O bonds closer to the lone pair site is seen in the structures of antimony β-diketonates such as $Sb(hfac)_3$ and $Sb(fod)_3$.[26]

Although 3-fold symmetry is absent in **3** (monoclinic $P2_1/n$), there are again three short and three long Sb−O interactions. The long bonds are all shorter than those seen in **2** [2.493−2.586 Å]; there is a similar range of distances for the short interactions [2.016−2.092 Å]. In both cases, there is no degree of association between individual molecules in the solid state.

Tin dialkylcarbamates have previously been reported and utilized to introduce tin onto a silica surface.[24] The structure of $Sn(O_2CNPr^i_2)_4$ has been briefly presented [24] but this alone represents the metrical data for such species. The structure of $Sn(O_2CNEt_2)_4$ (**4**) is shown in Figure 4 and is included here for comparison with the analogous Sb(III) species. The tin is eight-coordinated with each of the carbamates chelating tin in a symmetrical manner [Sn−O = 2.156(1)−2.209(1) Å; cf. $Sn(O_2CNPr^i_2)_4$ = 2.123(4)−2.218(4) Å],[24] reflecting both the greater Lewis acidity of Sn(IV) over Sb(III) and the absence of a lone pair to distort the metal coordination sphere. Compound **4** does not fit easily into any description based on a regular polyhedron, but can be viewed as a distorted square antiprism in which O(1)−O(4) and O(1′)−O(4′) make up opposing faces (Figure 4, bottom). No angular data have been reported for $Sn(O_2CNPr^i_2)_4$, but $Ti(O_2CNPr^i_2)_4$ adopts a dodecahedral arrangement distorted slightly from ideal D_{2d} and is cited as being isomorphous with the tin compound.[22]

All four compounds show good solubility in common organic solvents, which is a prerequisite for use as precursor in aerosol-assisted chemical vapor deposition experiments. The decomposition profiles of **1** and **4** are shown in Figure 5; thermal decompositions of **2** and **3** closely resemble that of **1**. Despite extended drying under vacuum, **1** loses weight rapidly on exposure to air, before showing a steady weight loss in the range 25−275 °C. Weight loss is effectively complete by 350 °C, though at this point the final residue (50%) is much higher than that expected for Sb_2O_3 (37.6%); the result is, however, compromised by the unquantifiable decomposition on loading the sample. Powder XRD on the residue (Figure 6) can be indexed to Sb_2O_3 thus confirming the nature of the final decomposition product; the residual organic matter remaining is low (C: 0.7, H: 0.1, N: 0.0%). Compound **4** also loses weight continuously between room

(25) Hall, M.; Sowerby, D. B. *J. Chem. Soc., Dalton Trans.* **1980**, 1292.

(26) Horley, G. A.; Mahon, M. F.; Molloy, K. C. Unpublished results.

temperature and *ca.* 300 °C, but displays a cleaner decomposition profile, and the final residue (*ca.* 28%) is close to that expected for SnO_2 (26%).

Compound **1** has been used as a precursor for the deposition of antimony oxide under LPCVD conditions. Sufficient volatility can be achieved at a precursor temperature of 130 °C at 10^{-2} Torr and a good quality film obtained at a decomposition temperature of 380 °C. The film is highly crystalline (Figure 7) and has been shown by X-ray diffraction to correspond to the senarmonite form of Sb_2O_3 (Figure 8). EDAX analysis of the film confirms the presence of both antimony and oxygen. We have previously grown a similar film from $Sb(OBu^n)_3$ at atmospheric pressure and 650 °C. While a similar (111) texture is seen in both cases, the crystal size from **1** (*ca.* 1 μm) is generally smaller than that from $Sb(OBu^n)_3$ (*ca.* 1−10 μm).[13]

Conclusions

Antimony dialkylcarbamates can be easily synthesized and, despite their sensitivity to moist air, are sufficiently volatile to be used as single-source precursors for the low-pressure CVD of Sb_2O_3 thin films. $Sn(O_2CNEt_2)_4$ shows a clean decomposition profile and is a possible single-source precursor for SnO_2.

Acknowledgment. This work was supported financially by the EPSRC, EpiChem, and Trolex. JREI/EPSRC is also thanked for funding the purchase of the diffractometer.

Supporting Information Available: Three X-ray Crystallographic files in CIF format. This material is available free of charge via the Internet at http://pubs.acs.org.

IC0202716